



Observation of excited Λ_b^0 baryons

The LHCb collaboration [†]

Abstract

Using pp collision data corresponding to 1.0 fb^{-1} integrated luminosity collected by the LHCb detector, two narrow states are observed in the $\Lambda_b^0 \pi^+ \pi^-$ spectrum with masses $5911.97 \pm 0.12(\text{stat}) \pm 0.02(\text{syst}) \pm 0.66(\Lambda_b^0 \text{ mass}) \text{ MeV}/c^2$ and $5919.77 \pm 0.08(\text{stat}) \pm 0.02(\text{syst}) \pm 0.66(\Lambda_b^0 \text{ mass}) \text{ MeV}/c^2$. The significances of the observations are 5.2 and 10.2 standard deviations, respectively. These states are interpreted as the orbitally excited Λ_b^0 baryons, $\Lambda_b^{*0}(5912)$ and $\Lambda_b^{*0}(5920)$.

To be submitted to Phys. Rev. Lett.

[†]Authors are listed on the following pages.

The LHCb collaboration

R. Aaij³⁸, C. Abellan Beteta^{33,n}, A. Adametz¹¹, B. Adeva³⁴, M. Adinolfi⁴³, C. Adrover⁶, A. Affolder⁴⁹, Z. Ajaltouni⁵, J. Albrecht³⁵, F. Alessio³⁵, M. Alexander⁴⁸, S. Ali³⁸, G. Alkhazov²⁷, P. Alvarez Cartelle³⁴, A.A. Alves Jr²², S. Amato², Y. Amhis³⁶, J. Anderson³⁷, R.B. Appleby⁵¹, O. Aquines Gutierrez¹⁰, F. Archilli^{18,35}, A. Artamonov³², M. Artuso^{53,35}, E. Aslanides⁶, G. Auriemma^{22,m}, S. Bachmann¹¹, J.J. Back⁴⁵, V. Balagura^{28,35}, W. Baldini¹⁶, R.J. Barlow⁵¹, C. Barschel³⁵, S. Barsuk⁷, W. Barter⁴⁴, A. Bates⁴⁸, C. Bauer¹⁰, Th. Bauer³⁸, A. Bay³⁶, J. Beddow⁴⁸, I. Bediaga¹, S. Belogurov²⁸, K. Belous³², I. Belyaev²⁸, E. Ben-Haim⁸, M. Benayoun⁸, G. Bencivenni¹⁸, S. Benson⁴⁷, J. Benton⁴³, R. Bernet³⁷, M.-O. Bettler¹⁷, M. van Beuzekom³⁸, A. Bien¹¹, S. Bifani¹², T. Bird⁵¹, A. Bizzeti^{17,h}, P.M. Bjørnstad⁵¹, T. Blake³⁵, F. Blanc³⁶, C. Blanks⁵⁰, J. Blouw¹¹, S. Blusk⁵³, A. Bobrov³¹, V. Bocci²², A. Bondar³¹, N. Bondar²⁷, W. Bonivento¹⁵, S. Borghi^{48,51}, A. Borgia⁵³, T.J.V. Bowcock⁴⁹, C. Bozzi¹⁶, T. Brambach⁹, J. van den Brand³⁹, J. Bressieux³⁶, D. Brett⁵¹, M. Britsch¹⁰, T. Britton⁵³, N.H. Brook⁴³, H. Brown⁴⁹, A. Büchler-Germann³⁷, I. Burducea²⁶, A. Bursche³⁷, J. Buytaert³⁵, S. Cadeddu¹⁵, O. Callot⁷, M. Calvi^{20,j}, M. Calvo Gomez^{33,n}, A. Camboni³³, P. Campana^{18,35}, A. Carbone¹⁴, G. Carboni^{21,k}, R. Cardinale^{19,i,35}, A. Cardini¹⁵, L. Carson⁵⁰, K. Carvalho Akiba², G. Casse⁴⁹, M. Cattaneo³⁵, Ch. Cauet⁹, M. Charles⁵², Ph. Charpentier³⁵, P. Chen^{3,36}, N. Chiapolini³⁷, M. Chrzaszcz²³, K. Ciba³⁵, X. Cid Vidal³⁴, G. Ciezarek⁵⁰, P.E.L. Clarke⁴⁷, M. Clemencic³⁵, H.V. Cliff⁴⁴, J. Closier³⁵, C. Coca²⁶, V. Coco³⁸, J. Cogan⁶, E. Cogneras⁵, P. Collins³⁵, A. Comerma-Montells³³, A. Contu⁵², A. Cook⁴³, M. Coombes⁴³, G. Corti³⁵, B. Couturier³⁵, G.A. Cowan³⁶, D. Craik⁴⁵, R. Currie⁴⁷, C. D'Ambrosio³⁵, P. David⁸, P.N.Y. David³⁸, I. De Bonis⁴, K. De Bruyn³⁸, S. De Capua^{21,k}, M. De Cian³⁷, J.M. De Miranda¹, L. De Paula², P. De Simone¹⁸, D. Decamp⁴, M. Deckenhoff⁹, H. Degaudenzi^{36,35}, L. Del Buono⁸, C. Deplano¹⁵, D. Derkach^{14,35}, O. Deschamps⁵, F. Dettori³⁹, J. Dickens⁴⁴, H. Dijkstra³⁵, P. Diniz Batista¹, F. Domingo Bonal^{33,n}, S. Donleavy⁴⁹, F. Dordei¹¹, A. Dosil Suárez³⁴, D. Dossett⁴⁵, A. Dovbnya⁴⁰, F. Dupertuis³⁶, R. Dzhelyadin³², A. Dziurda²³, A. Dzyuba²⁷, S. Easo⁴⁶, U. Egede⁵⁰, V. Egorychev²⁸, S. Eidelman³¹, D. van Eijk³⁸, F. Eisele¹¹, S. Eisenhardt⁴⁷, R. Ekelhof⁹, L. Eklund⁴⁸, I. El Rifai⁵, Ch. Elsasser³⁷, D. Elsby⁴², D. Esperante Pereira³⁴, A. Falabella^{16,e,14}, C. Färber¹¹, G. Fardell⁴⁷, C. Farinelli³⁸, S. Farry¹², V. Fave³⁶, V. Fernandez Albor³⁴, M. Ferro-Luzzi³⁵, S. Filippov³⁰, C. Fitzpatrick⁴⁷, M. Fontana¹⁰, F. Fontanelli^{19,i}, R. Forty³⁵, O. Francisco², M. Frank³⁵, C. Frei³⁵, M. Frosini^{17,f}, S. Furcas²⁰, A. Gallas Torreira³⁴, D. Galli^{14,c}, M. Gandelman², P. Gandini⁵², Y. Gao³, J.-C. Garnier³⁵, J. Garofoli⁵³, J. Garra Tico⁴⁴, L. Garrido³³, D. Gascon³³, C. Gaspar³⁵, R. Gauld⁵², N. Gauvin³⁶, M. Gersabeck³⁵, T. Gershon^{45,35}, Ph. Ghez⁴, V. Gibson⁴⁴, V.V. Gligorov³⁵, C. Göbel⁵⁴, D. Golubkov²⁸, A. Golutvin^{50,28,35}, A. Gomes², H. Gordon⁵², M. Grabalosa Gándara³³, R. Graciani Diaz³³, L.A. Granado Cardoso³⁵, E. Graugés³³, G. Graziani¹⁷, A. Grecu²⁶, E. Greening⁵², S. Gregson⁴⁴, O. Grünberg⁵⁵, B. Gui⁵³, E. Gushchin³⁰, Yu. Guz³², T. Gys³⁵, C. Hadjivasiliou⁵³, G. Haefeli³⁶, C. Haen³⁵, S.C. Haines⁴⁴, T. Hampson⁴³, S. Hansmann-Menzemer¹¹, N. Harnew⁵², S.T. Harnew⁴³, J. Harrison⁵¹, P.F. Harrison⁴⁵, T. Hartmann⁵⁵, J. He⁷, V. Heijne³⁸, K. Hennessy⁴⁹, P. Henrard⁵, J.A. Hernando Morata³⁴, E. van Herwijnen³⁵, E. Hicks⁴⁹, M. Hoballah⁵, P. Hopchev⁴, W. Hulsbergen³⁸, P. Hunt⁵², T. Huse⁴⁹, R.S. Huston¹², D. Hutchcroft⁴⁹, D. Hynds⁴⁸, V. Iakovenko⁴¹, P. Ilten¹², J. Imong⁴³, R. Jacobsson³⁵, A. Jaeger¹¹, M. Jahjah Hussein⁵, E. Jans³⁸, F. Jansen³⁸, P. Jaton³⁶, B. Jean-Marie⁷, F. Jing³, M. John⁵², D. Johnson⁵², C.R. Jones⁴⁴, B. Jost³⁵, M. Kabbalo⁹, S. Kandybei⁴⁰, M. Karacson³⁵,

T.M. Karbach⁹, J. Keaveney¹², I.R. Kenyon⁴², U. Kerzel³⁵, T. Ketel³⁹, A. Keune³⁶,
 B. Khanji⁶, Y.M. Kim⁴⁷, M. Knecht³⁶, O. Kochebina⁷, I. Komarov²⁹, R.F. Koopman³⁹,
 P. Koppenburg³⁸, M. Korolev²⁹, A. Kozlinskiy³⁸, L. Kravchuk³⁰, K. Kreplin¹¹, M. Kreps⁴⁵,
 G. Krocker¹¹, P. Krokovny³¹, F. Kruse⁹, K. Kruzelecki³⁵, M. Kucharczyk^{20,23,35,j},
 V. Kudryavtsev³¹, T. Kvaratskheliya^{28,35}, V.N. La Thi³⁶, D. Lacarrere³⁵, G. Lafferty⁵¹,
 A. Lai¹⁵, D. Lambert⁴⁷, R.W. Lambert³⁹, E. Lanciotti³⁵, G. Lanfranchi¹⁸, C. Langenbruch³⁵,
 T. Latham⁴⁵, C. Lazzeroni⁴², R. Le Gac⁶, J. van Leerdam³⁸, J.-P. Lees⁴, R. Lefèvre⁵,
 A. Leflat^{29,35}, J. Lefrançois⁷, O. Leroy⁶, T. Lesiak²³, L. Li³, Y. Li³, L. Li Gioi⁵, M. Lieng⁹,
 M. Liles⁴⁹, R. Lindner³⁵, C. Linn¹¹, B. Liu³, G. Liu³⁵, J. von Loeben²⁰, J.H. Lopes²,
 E. Lopez Asamar³³, N. Lopez-March³⁶, H. Lu³, J. Luisier³⁶, A. Mac Raighne⁴⁸, F. Machefert⁷,
 I.V. Machikhiliyan^{4,28}, F. Maciuc¹⁰, O. Maev^{27,35}, J. Magnin¹, S. Malde⁵²,
 R.M.D. Mamunur³⁵, G. Manca^{15,d}, G. Mancinelli⁶, N. Mangiafave⁴⁴, U. Marconi¹⁴, R. Märki³⁶,
 J. Marks¹¹, G. Martellotti²², A. Martens⁸, L. Martin⁵², A. Martín Sánchez⁷, M. Martinelli³⁸,
 D. Martinez Santos³⁵, A. Massafferri¹, Z. Mathe¹², C. Matteuzzi²⁰, M. Matveev²⁷,
 E. Maurice⁶, B. Maynard⁵³, A. Mazurov^{16,30,35}, J. McCarthy⁴², G. McGregor⁵¹, R. McNulty¹²,
 M. Meissner¹¹, M. Merk³⁸, J. Merkel⁹, D.A. Milanese¹³, M.-N. Minard⁴, J. Molina Rodriguez⁵⁴,
 S. Monteil⁵, D. Moran¹², P. Morawski²³, R. Mountain⁵³, I. Mous³⁸, F. Muheim⁴⁷, K. Müller³⁷,
 R. Muresan²⁶, B. Muryn²⁴, B. Muster³⁶, J. Mylroie-Smith⁴⁹, P. Naik⁴³, T. Nakada³⁶,
 R. Nandakumar⁴⁶, I. Nasteva¹, M. Needham⁴⁷, N. Neufeld³⁵, A.D. Nguyen³⁶,
 C. Nguyen-Mau^{36,o}, M. Nicol⁷, V. Niess⁵, N. Nikitin²⁹, T. Nikodem¹¹, A. Nomerotski^{52,35},
 A. Novoselov³², A. Oblakowska-Mucha²⁴, V. Obraztsov³², S. Oggero³⁸, S. Ogilvy⁴⁸,
 O. Okhrimenko⁴¹, R. Oldeman^{15,d,35}, M. Orlandea²⁶, J.M. Otalora Goicochea², P. Owen⁵⁰,
 B.K. Pal⁵³, J. Palacios³⁷, A. Palano^{13,b}, M. Palutan¹⁸, J. Panman³⁵, A. Papanestis⁴⁶,
 M. Pappagallo⁴⁸, C. Parkes⁵¹, C.J. Parkinson⁵⁰, G. Passaleva¹⁷, G.D. Patel⁴⁹, M. Patel⁵⁰,
 G.N. Patrick⁴⁶, C. Patrignani^{19,i}, C. Pavel-Nicorescu²⁶, A. Pazos Alvarez³⁴, A. Pellegrino³⁸,
 G. Penso^{22,l}, M. Pepe Altarelli³⁵, S. Perazzini^{14,c}, D.L. Perego^{20,j}, E. Perez Trigo³⁴,
 A. Pérez-Calero Yzquierdo³³, P. Perret⁵, M. Perrin-Terrin⁶, G. Pessina²⁰, A. Petrolini^{19,i},
 A. Phan⁵³, E. Picatoste Olloqui³³, B. Pie Valls³³, B. Pietrzyk⁴, T. Pilař⁴⁵, D. Pinci²²,
 R. Plackett⁴⁸, S. Playfer⁴⁷, M. Plo Casasus³⁴, F. Polci⁸, G. Polok²³, A. Poluektov^{45,31},
 E. Polcarpo², D. Popov¹⁰, B. Popovici²⁶, C. Potterat³³, A. Powell⁵², J. Prisciandaro³⁶,
 V. Pugatch⁴¹, A. Puig Navarro³³, W. Qian⁵³, J.H. Rademacker⁴³, B. Rakotomiaramanana³⁶,
 M.S. Rangel², I. Raniuk⁴⁰, G. Raven³⁹, S. Redford⁵², M.M. Reid⁴⁵, A.C. dos Reis¹,
 S. Ricciardi⁴⁶, A. Richards⁵⁰, K. Rinnert⁴⁹, D.A. Roa Romero⁵, P. Robbe⁷, E. Rodrigues^{48,51},
 F. Rodrigues², P. Rodriguez Perez³⁴, G.J. Rogers⁴⁴, S. Roiser³⁵, V. Romanovsky³²,
 M. Rosello^{33,n}, J. Rouvinet³⁶, T. Ruf³⁵, H. Ruiz³³, G. Sabatino^{21,k}, J.J. Saborido Silva³⁴,
 N. Sagidova²⁷, P. Sail⁴⁸, B. Saitta^{15,d}, C. Salzmann³⁷, B. Sanmartin Sedes³⁴, M. Sannino^{19,i},
 R. Santacesaria²², C. Santamarina Rios³⁴, R. Santinelli³⁵, E. Santovetti^{21,k}, M. Sapunov⁶,
 A. Sarti^{18,l}, C. Satriano^{22,m}, A. Satta²¹, M. Savrie^{16,e}, D. Savrina²⁸, P. Schaack⁵⁰,
 M. Schiller³⁹, H. Schindler³⁵, S. Schleich⁹, M. Schlupp⁹, M. Schmelling¹⁰, B. Schmidt³⁵,
 O. Schneider³⁶, A. Schopper³⁵, M.-H. Schune⁷, R. Schwemmer³⁵, B. Sciascia¹⁸, A. Sciubba^{18,l},
 M. Seco³⁴, A. Semennikov²⁸, K. Senderowska²⁴, I. Sepp⁵⁰, N. Serra³⁷, J. Serrano⁶, P. Seyfert¹¹,
 M. Shapkin³², I. Shapoval^{40,35}, P. Shatalov²⁸, Y. Shcheglov²⁷, T. Shears⁴⁹, L. Shekhtman³¹,
 O. Shevchenko⁴⁰, V. Shevchenko²⁸, A. Shires⁵⁰, R. Silva Coutinho⁴⁵, T. Skwarnicki⁵³,
 N.A. Smith⁴⁹, E. Smith^{52,46}, M. Smith⁵¹, K. Sobczak⁵, F.J.P. Soler⁴⁸, A. Solomin⁴³,
 F. Soomro^{18,35}, D. Souza⁴³, B. Souza De Paula², B. Spaan⁹, A. Sparkes⁴⁷, P. Spradlin⁴⁸,
 F. Stagni³⁵, S. Stahl¹¹, O. Steinkamp³⁷, S. Stoica²⁶, S. Stone^{53,35}, B. Storaci³⁸, M. Straticiuc²⁶,

U. Straumann³⁷, V.K. Subbiah³⁵, S. Swientek⁹, M. Szczekowski²⁵, P. Szczypka³⁶,
T. Szumlak²⁴, S. T'Jampens⁴, M. Teklishyn⁷, E. Teodorescu²⁶, F. Teubert³⁵, C. Thomas⁵²,
E. Thomas³⁵, J. van Tilburg¹¹, V. Tisserand⁴, M. Tobin³⁷, S. Tolks³⁹, S. Topp-Joergensen⁵²,
N. Torr⁵², E. Tournefier^{4,50}, S. Tourneur³⁶, M.T. Tran³⁶, A. Tsaregorodtsev⁶, N. Tuning³⁸,
M. Ubeda Garcia³⁵, A. Ukleja²⁵, U. Uwer¹¹, V. Vagnoni¹⁴, G. Valenti¹⁴, R. Vazquez Gomez³³,
P. Vazquez Regueiro³⁴, S. Vecchi¹⁶, J.J. Velthuis⁴³, M. Veltri^{17,9}, M. Vesterinen³⁵, B. Viaud⁷,
I. Videau⁷, D. Vieira², X. Vilasis-Cardona^{33,n}, J. Visniakov³⁴, A. Vollhardt³⁷, D. Volyanskyy¹⁰,
D. Voong⁴³, A. Vorobyev²⁷, V. Vorobyev³¹, C. Vof⁵⁵, H. Voss¹⁰, R. Waldi⁵⁵, R. Wallace¹²,
S. Wandernoth¹¹, J. Wang⁵³, D.R. Ward⁴⁴, N.K. Watson⁴², A.D. Webber⁵¹, D. Websdale⁵⁰,
M. Whitehead⁴⁵, J. Wicht³⁵, D. Wiedner¹¹, L. Wiggers³⁸, G. Wilkinson⁵², M.P. Williams^{45,46},
M. Williams⁵⁰, F.F. Wilson⁴⁶, J. Wishahi⁹, M. Witek²³, W. Witzeling³⁵, S.A. Wotton⁴⁴,
S. Wright⁴⁴, S. Wu³, K. Wyllie³⁵, Y. Xie⁴⁷, F. Xing⁵², Z. Xing⁵³, Z. Yang³, R. Young⁴⁷,
X. Yuan³, O. Yushchenko³², M. Zangoli¹⁴, M. Zavertyaev^{10,a}, F. Zhang³, L. Zhang⁵³,
W.C. Zhang¹², Y. Zhang³, A. Zhelezov¹¹, L. Zhong³, A. Zvyagin³⁵.

¹ *Centro Brasileiro de Pesquisas Físicas (CBPF), Rio de Janeiro, Brazil*

² *Universidade Federal do Rio de Janeiro (UFRJ), Rio de Janeiro, Brazil*

³ *Center for High Energy Physics, Tsinghua University, Beijing, China*

⁴ *LAPP, Université de Savoie, CNRS/IN2P3, Annecy-Le-Vieux, France*

⁵ *Clermont Université, Université Blaise Pascal, CNRS/IN2P3, LPC, Clermont-Ferrand, France*

⁶ *CPPM, Aix-Marseille Université, CNRS/IN2P3, Marseille, France*

⁷ *LAL, Université Paris-Sud, CNRS/IN2P3, Orsay, France*

⁸ *LPNHE, Université Pierre et Marie Curie, Université Paris Diderot, CNRS/IN2P3, Paris, France*

⁹ *Fakultät Physik, Technische Universität Dortmund, Dortmund, Germany*

¹⁰ *Max-Planck-Institut für Kernphysik (MPIK), Heidelberg, Germany*

¹¹ *Physikalisches Institut, Ruprecht-Karls-Universität Heidelberg, Heidelberg, Germany*

¹² *School of Physics, University College Dublin, Dublin, Ireland*

¹³ *Sezione INFN di Bari, Bari, Italy*

¹⁴ *Sezione INFN di Bologna, Bologna, Italy*

¹⁵ *Sezione INFN di Cagliari, Cagliari, Italy*

¹⁶ *Sezione INFN di Ferrara, Ferrara, Italy*

¹⁷ *Sezione INFN di Firenze, Firenze, Italy*

¹⁸ *Laboratori Nazionali dell'INFN di Frascati, Frascati, Italy*

¹⁹ *Sezione INFN di Genova, Genova, Italy*

²⁰ *Sezione INFN di Milano Bicocca, Milano, Italy*

²¹ *Sezione INFN di Roma Tor Vergata, Roma, Italy*

²² *Sezione INFN di Roma La Sapienza, Roma, Italy*

²³ *Henryk Niewodniczanski Institute of Nuclear Physics Polish Academy of Sciences, Kraków, Poland*

²⁴ *AGH University of Science and Technology, Kraków, Poland*

²⁵ *Soltan Institute for Nuclear Studies, Warsaw, Poland*

²⁶ *Horia Hulubei National Institute of Physics and Nuclear Engineering, Bucharest-Magurele, Romania*

²⁷ *Petersburg Nuclear Physics Institute (PNPI), Gatchina, Russia*

²⁸ *Institute of Theoretical and Experimental Physics (ITEP), Moscow, Russia*

²⁹ *Institute of Nuclear Physics, Moscow State University (SINP MSU), Moscow, Russia*

³⁰ *Institute for Nuclear Research of the Russian Academy of Sciences (INR RAN), Moscow, Russia*

³¹ *Budker Institute of Nuclear Physics (SB RAS) and Novosibirsk State University, Novosibirsk, Russia*

³² *Institute for High Energy Physics (IHEP), Protvino, Russia*

³³ *Universitat de Barcelona, Barcelona, Spain*

³⁴ *Universidad de Santiago de Compostela, Santiago de Compostela, Spain*

³⁵ *European Organization for Nuclear Research (CERN), Geneva, Switzerland*

- ³⁶ *Ecole Polytechnique Fédérale de Lausanne (EPFL), Lausanne, Switzerland*
- ³⁷ *Physik-Institut, Universität Zürich, Zürich, Switzerland*
- ³⁸ *Nikhef National Institute for Subatomic Physics, Amsterdam, The Netherlands*
- ³⁹ *Nikhef National Institute for Subatomic Physics and VU University Amsterdam, Amsterdam, The Netherlands*
- ⁴⁰ *NSC Kharkiv Institute of Physics and Technology (NSC KIPT), Kharkiv, Ukraine*
- ⁴¹ *Institute for Nuclear Research of the National Academy of Sciences (KINR), Kyiv, Ukraine*
- ⁴² *University of Birmingham, Birmingham, United Kingdom*
- ⁴³ *H.H. Wills Physics Laboratory, University of Bristol, Bristol, United Kingdom*
- ⁴⁴ *Cavendish Laboratory, University of Cambridge, Cambridge, United Kingdom*
- ⁴⁵ *Department of Physics, University of Warwick, Coventry, United Kingdom*
- ⁴⁶ *STFC Rutherford Appleton Laboratory, Didcot, United Kingdom*
- ⁴⁷ *School of Physics and Astronomy, University of Edinburgh, Edinburgh, United Kingdom*
- ⁴⁸ *School of Physics and Astronomy, University of Glasgow, Glasgow, United Kingdom*
- ⁴⁹ *Oliver Lodge Laboratory, University of Liverpool, Liverpool, United Kingdom*
- ⁵⁰ *Imperial College London, London, United Kingdom*
- ⁵¹ *School of Physics and Astronomy, University of Manchester, Manchester, United Kingdom*
- ⁵² *Department of Physics, University of Oxford, Oxford, United Kingdom*
- ⁵³ *Syracuse University, Syracuse, NY, United States*
- ⁵⁴ *Pontifícia Universidade Católica do Rio de Janeiro (PUC-Rio), Rio de Janeiro, Brazil, associated to ²*
- ⁵⁵ *Institut für Physik, Universität Rostock, Rostock, Germany, associated to ¹¹*
- ^a *P.N. Lebedev Physical Institute, Russian Academy of Science (LPI RAS), Moscow, Russia*
- ^b *Università di Bari, Bari, Italy*
- ^c *Università di Bologna, Bologna, Italy*
- ^d *Università di Cagliari, Cagliari, Italy*
- ^e *Università di Ferrara, Ferrara, Italy*
- ^f *Università di Firenze, Firenze, Italy*
- ^g *Università di Urbino, Urbino, Italy*
- ^h *Università di Modena e Reggio Emilia, Modena, Italy*
- ⁱ *Università di Genova, Genova, Italy*
- ^j *Università di Milano Bicocca, Milano, Italy*
- ^k *Università di Roma Tor Vergata, Roma, Italy*
- ^l *Università di Roma La Sapienza, Roma, Italy*
- ^m *Università della Basilicata, Potenza, Italy*
- ⁿ *LIFAEELS, La Salle, Universitat Ramon Llull, Barcelona, Spain*
- ^o *Hanoi University of Science, Hanoi, Viet Nam*

1 The system of baryons containing a b quark (beauty baryons) remains largely unex-
 2 plored, despite recent progress made at the experiments at the Tevatron. In addition to
 3 the ground state, Λ_b^0 , the Ξ_b^- baryon with the quark content bsd has been observed by
 4 the D0 [1] and CDF [2] collaborations, followed by the observation of the doubly-strange
 5 Ω_b^- baryon (bsb) [3, 4]. The last ground state of beauty-strange content, Ξ_b^0 (bsu), has
 6 been observed by CDF [5]. Recently, the CMS collaboration has found the corresponding
 7 excited state, most likely Ξ_b^{*0} with $J^P = 3/2^+$ [6]. Beauty baryons with two light quarks
 8 (bqq , where $q = u, d$), other than the Λ_b^0 , have been studied so far by CDF only. Of the
 9 triplets $\Sigma_b^{\pm,0}$ with spin $J = 1/2$ and $\Sigma_b^{*\pm,0}$ with $J = 3/2$ predicted by theory, only the
 10 charged states $\Sigma_b^{(*)\pm}$ have so far been observed via their decay to $\Lambda_b^0\pi^\pm$ final states [7, 8].
 11 None of the quantum numbers of beauty baryons have been measured.

12 The quark model predicts the existence of two orbitally excited Λ_b^0 states, Λ_b^{*0} , with
 13 the quantum numbers $J^P = 1/2^-$ and $3/2^-$, respectively, that should decay to $\Lambda_b^0\pi^+\pi^-$ or
 14 $\Lambda_b^0\gamma$. These states have not previously been established experimentally. The properties of
 15 excited Λ_b^0 baryons are discussed in Refs. [9–15]. Most predictions give masses above the
 16 $\Lambda_b^0\pi^+\pi^-$ threshold, but below the $\Sigma_b\pi$ threshold. Observation of Λ_b^{*0} states and measure-
 17 ment of their quantum numbers would provide a further confirmation of the validity of
 18 the quark model, and the precise measurement of their masses would test the applicability
 19 of various theoretical models used to describe the interaction of heavy quarks.

20 This Letter reports the first observation of the Λ_b^{*0} states decaying into $\Lambda_b^0\pi^+\pi^-$, and
 21 the measurement of their masses and upper limits on their natural widths. The data
 22 set of 1.0 fb^{-1} collected in pp collisions at the LHC collider at the center-of-mass energy
 23 $\sqrt{s} = 7 \text{ TeV}$ in 2011 is used for the analysis.

24 The LHCb detector [16] is a single-arm forward spectrometer covering the pseudo-
 25 rapidity range $2 < \eta < 5$, designed for the study of particles containing b or c quarks.
 26 The detector includes a high precision tracking system consisting of a silicon-strip vertex
 27 detector surrounding the pp interaction region, a large-area silicon-strip detector located
 28 upstream of a dipole magnet with a bending power of about 4 Tm, and three stations
 29 of silicon-strip detectors and straw drift tubes placed downstream. The combined track-
 30 ing system has a momentum resolution $\Delta p/p$ that varies from 0.4% at 5 GeV/ c to 0.6%
 31 at 100 GeV/ c , and an impact parameter (IP) resolution of 20 μm for tracks with high
 32 transverse momentum. Charged hadrons are identified using two ring-imaging Cherenkov
 33 (RICH) detectors. Photon, electron and hadron candidates are identified by a calorime-
 34 ter system consisting of scintillating-pad and preshower detectors, an electromagnetic
 35 calorimeter and a hadronic calorimeter. Muons are identified by a muon system com-
 36 posed of alternating layers of iron and multiwire proportional chambers.

37 The online event selection (trigger) consists of a hardware stage, based on information
 38 from the calorimeter and muon systems, followed by a software stage which applies full
 39 event reconstruction. The software trigger used in this analysis requires a two-, three- or
 40 four-track secondary vertex with a high sum of the momenta transverse to the beam axis,
 41 p_T , of the tracks, and significant displacement from the primary interaction vertex (PV).
 42 In addition, the secondary vertex should have at least one track with $p_T > 1.7 \text{ GeV}/c$, IP
 43 χ^2 with respect to any PV greater than 16 (where the IP χ^2 is defined as the difference

44 of the PV fit χ^2 with and without the track included), and a track fit $\chi^2/\text{ndf} < 2$ where
 45 ndf is the number of degrees of freedom in the fit. A multivariate algorithm is used for
 46 the identification of the secondary vertices [17].

47 The Λ_b^0 candidates are reconstructed in the $\Lambda_b^0 \rightarrow \Lambda_c^+ \pi^-$, $\Lambda_c^+ \rightarrow p K^- \pi^+$ decay chain
 48 (addition of charge-conjugate states is implied throughout this Letter). The selection of
 49 Λ_b^0 candidates is performed in two stages. First, a loose preselection of events containing
 50 beauty hadron candidates decaying to charm hadron candidates is performed. It requires
 51 that the tracks forming the candidate, as well as the beauty and charm vertices, have
 52 good quality and are well separated from any PV, and the invariant masses of the beauty
 53 and charm candidates are consistent with the masses of the corresponding particles.

54 The final selection requires that all the tracks forming the Λ_b^0 candidate have an IP
 55 χ^2 with respect to any PV greater than 9, and the IP χ^2 of the Λ_b^0 candidate to the
 56 best PV (PV having the minimum IP χ^2 for the Λ_b^0 candidate) is less than 16. Particle
 57 identification (PID) information from the RICH detectors is used to identify kaons and
 58 protons in the final state in the form of differences of logarithms of likelihoods between the
 59 proton and pion ($\text{DLL}_{p\pi}$) and kaon and pion ($\text{DLL}_{K\pi}$) hypotheses. No PID requirements
 60 are applied to the pions from $\Lambda_b^0 \rightarrow \Lambda_c^+ \pi^-$ decays to increase the Λ_b^0 yield: a significant
 61 fraction of these pions have momenta above 100 GeV/ c where the PID performance is
 62 reduced. Finally, a kinematic fit is used which constrains the decay products of the Λ_b^0
 63 and Λ_c^+ baryons to originate from common vertices, the Λ_b^0 to originate from the PV and
 64 the invariant mass of the Λ_c^+ candidate to be equal to the established Λ_c^+ mass [18].

65 A momentum scale correction is applied to all invariant mass spectra in this analysis
 66 to improve the mass measurement using the procedure similar to [19]. The momentum
 67 scale has been calibrated using $J/\psi \rightarrow \mu^+ \mu^-$ decays, and its accuracy has been quantified
 68 with other two-body resonance decays ($\Upsilon(1S) \rightarrow \mu^+ \mu^-$, $K_s^0 \rightarrow \pi^+ \pi^-$, $\phi \rightarrow K^+ K^-$).

69 Signal and background distributions are studied using simulation. Proton-proton collisions
 70 are generated using PYTHIA 6.4 [20] with a specific LHCb configuration [21]. Decays
 71 of hadronic particles are described by EVTGEN [22] in which final state radiation is gener-
 72 ated using PHOTOS [23]. The interaction of the generated particles with the detector
 73 and its response are implemented using the GEANT4 toolkit [24] as described in Ref. [25].

74 The distribution of the $\Lambda_c^+ \pi^-$ invariant mass after the kinematic fit is shown in Fig. 1,
 75 where a requirement of good quality of the kinematic fit is applied. In addition to the $\Lambda_b^0 \rightarrow$
 76 $\Lambda_c^+ \pi^-$ signal contribution, the spectrum contains backgrounds from random combinations
 77 of tracks (random background), from partially-reconstructed decays where one or more
 78 particles are not reconstructed, and from $\Lambda_b^0 \rightarrow \Lambda_c^+ K^-$ decays with the kaon reconstructed
 79 under the pion mass hypothesis. A fit of the spectrum yields $70\,540 \pm 330$ signal events,
 80 and the signal-to-background ratio in a ± 25 MeV/ c^2 interval around the nominal Λ_b^0 mass
 81 is $S/B = 11$. The fit to the $\Lambda_c^+ \pi^-$ spectrum is only used to estimate the Λ_b^0 yield and the
 82 $\Lambda_b^0 \rightarrow \Lambda_c^+ K^-$ contribution, and is not used in the subsequent analysis.

83 The Λ_b^0 candidates obtained with the above selection are combined with two tracks under
 84 the pion mass hypothesis (referred to as slow pions from now on) to search for excited
 85 Λ_b^0 states. The tracks are required to have transverse momentum $p_T > 150$ MeV/ c , and no
 86 PID requirements are applied. A kinematic fit is applied that, in addition to all constraints

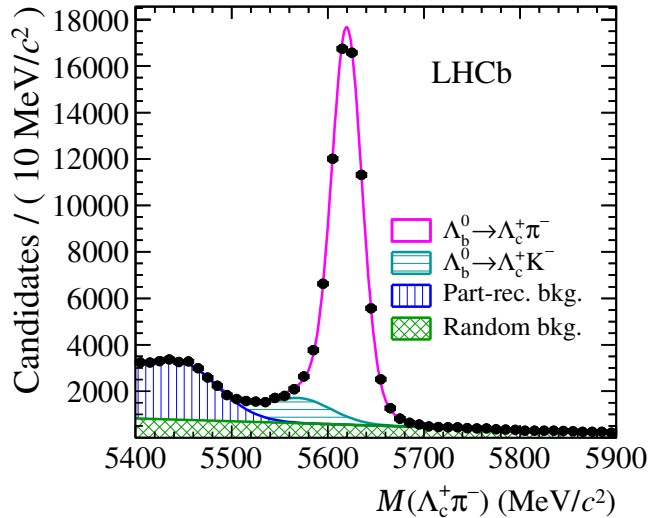


Figure 1: Invariant mass spectrum of $\Lambda_c^+\pi^-$ combinations. The points with error bars are the data, and the fitted $\Lambda_b^0 \rightarrow \Lambda_c^+\pi^-$ signal and three background components ($\Lambda_b^0 \rightarrow \Lambda_c^+K^-$, partially-reconstructed and random background) are shown with different fill styles.

87 described above for Λ_b^0 candidates, constrains the two slow pion tracks to originate from
 88 the PV and the invariant mass of the Λ_b^0 candidate to a fixed value of $5619.37 \text{ MeV}/c^2$,
 89 which is a combination of the world average [18] and the LHCb measurement [26]. The
 90 uncertainty on the combined Λ_b^0 mass obtained in this way, $0.69 \text{ MeV}/c^2$, is treated as a
 91 systematic effect. Combinations with a good quality of kinematic fit, $\chi^2/\text{ndf} < 3.3$, are
 92 retained. From the simulation study, this requirement is optimal for the observation of a
 93 narrow state near the kinematic threshold with signal-to-background ratio around one.

94 The fit of the $\Lambda_c^+\pi^-$ mass spectrum (Fig. 1) indicates the presence of the background
 95 from $\Lambda_b^0 \rightarrow \Lambda_c^+K^-$ decays at a rate around 12%, relative to the $\Lambda_b^0 \rightarrow \Lambda_c^+\pi^-$ signal.
 96 Alternatively, its rate can be estimated from the ratio of $B^+ \rightarrow \bar{D}^0K^+$ and $B^+ \rightarrow \bar{D}^0\pi^+$
 97 decays that equals to 8% [18]. Due to the Λ_b^0 mass constraint in the kinematic fit, the
 98 $\Lambda_b^0\pi^+\pi^-$ invariant mass distribution for this mode is biased by less than $0.1 \text{ MeV}/c^2$ if
 99 reconstructed under the $\Lambda_c^+\pi^-$ mass hypothesis, and has a resolution only a factor of two
 100 worse than that with the $\Lambda_c^+\pi^-$ signal. After the kinematic fit quality requirement, the
 101 fraction of $\Lambda_b^0\pi^+\pi^-$ with $\Lambda_b^0 \rightarrow \Lambda_c^+K^-$ decays compared to those with the $\Lambda_c^+\pi^-$ is reduced
 102 to 8%. This mode is thus not treated separately, and its effect is taken into account as a
 103 part of the systematic uncertainty due to the signal shape.

104 Combinations of Λ_b^0 candidates with both opposite-sign and same-sign slow pions are
 105 selected in data. The latter are used to constrain the background shape coming from
 106 random combinations of Λ_b^0 baryon and two tracks. The assumption that the shape of the
 107 background in $\Lambda_b^0\pi^+\pi^-$ and $\Lambda_b^0\pi^\pm\pi^\pm$ modes is the same is validated with simulation. The
 108 $\Lambda_b^0\pi^+\pi^-$ and $\Lambda_b^0\pi^\pm\pi^\pm$ invariant mass spectra are shown in Fig. 2; two narrow structures
 109 with masses around 5912 and $5920 \text{ MeV}/c^2$ are evident in the $\Lambda_b^0\pi^+\pi^-$ spectrum. They

110 are interpreted as the orbitally excited A_b^0 states, and are denoted hereafter as $A_b^{*0}(5912)$
 111 and $A_b^{*0}(5920)$.

112 A combined unbinned fit of the $A_b^0\pi^+\pi^-$ and $A_b^0\pi^\pm\pi^\pm$ samples is performed to ex-
 113 tract the masses and event yields of the two states. The background is described with a
 114 quadratic polynomial function with common parameters for both samples except for an
 115 overall normalization. The probability density function (PDF) for each of the $A_b^{*0}(5912)$
 116 and $A_b^{*0}(5920)$ signals is a sum of two Gaussian PDFs with the same mean. The rela-
 117 tive normalization of the two Gaussian PDFs are fixed to the values obtained from the
 118 simulation of states with masses 5912 and 5920 MeV/ c^2 and zero natural widths, while
 119 the mean value and overall normalization for each signal are left free in the fit. The core
 120 resolution (width of the narrower Gaussian PDF) obtained from simulation is 0.19 and
 121 0.27 MeV/ c^2 for $A_b^{*0}(5912)$ and $A_b^{*0}(5920)$, respectively. Study of several high-statistics
 122 samples ($A_b^0 \rightarrow A_c^+\pi^-$, $\psi(2S) \rightarrow J/\psi\pi^+\pi^-$, $D^{*+} \rightarrow D^0\pi^+$) shows that the invariant mass
 123 resolution in data is typically worse by 20% than in the simulation. Thus the nominal data
 124 fit uses the widths of Gaussian PDFs from the simulation multiplied by 1.2. The data
 125 fit yields 17.6 ± 4.8 events with mass $M_{A_b^{*0}(5912)} = 5911.97 \pm 0.12$ MeV/ c^2 and 52.5 ± 8.1
 126 events with mass $M_{A_b^{*0}(5920)} = 5919.77 \pm 0.08$ MeV/ c^2 .

127 Limits on natural widths Γ of the two states are obtained by performing an alternative
 128 fit where the signal PDFs are convolved with relativistic Breit-Wigner distributions. The
 129 dependence of Breit-Wigner width Γ on the $A_b^0\pi^+\pi^-$ invariant mass M is taken into
 130 account as $\Gamma_{A_b^{*0}}(M) = \Gamma_{A_b^{*0}} \times (q/q_0)^2 \times (M_{A_b^{*0}}/M)$. Here $M_{A_b^{*0}}$ is the mass of the A_b^{*0}
 131 state, and $q_{(0)}$ is the kinematic energy for the decay of the state with mass $M_{(A_b^{*0})}$: $q_{(0)} =$
 132 $M_{(A_b^{*0})} - M_{A_b^0} - 2M_\pi$, where $M_{A_b^0}$ and M_π are the masses of A_b^0 and π^+ , respectively.
 133 Scans of Breit-Wigner widths $\Gamma_{A_b^{*0}(5912)}$ and $\Gamma_{A_b^{*0}(5920)}$ are performed with all the other
 134 parameters free to vary in the fit. The upper limits are obtained without applying the
 135 mass resolution scaling factor of 1.2 as in the nominal fit to account for the uncertainty
 136 of this quantity: this gives a more conservative value for the upper limit. The 90%
 137 (95%) confidence level (CL) upper limit on Γ , which corresponds to 1.28 (1.64) standard
 138 deviations, is obtained as the value of Γ where the negative logarithm of the likelihood
 139 is $1.28^2/2 = 0.82$ ($1.64^2/2 = 1.34$) greater than at its minimum. The 90% (95%) CL
 140 upper limit is $\Gamma_{A_b^{*0}(5912)} < 0.66$ MeV (0.83 MeV) for the $A_b^{*0}(5912)$ state, and $\Gamma_{A_b^{*0}(5920)} <$
 141 0.63 MeV (0.75 MeV) for the $A_b^{*0}(5920)$ state.

142 The invariant mass of the two pions, $M(\pi^+\pi^-)$, in the $A_b^{*0}(5920) \rightarrow A_b^0\pi^+\pi^-$ decay
 143 is shown in Fig. 3. The background is subtracted using the *sWeights* procedure [27].
 144 The weights are calculated from the fit to $A_b^0\pi^+\pi^-$ invariant mass distribution, which is
 145 practically uncorrelated with $M(\pi^+\pi^-)$. The $M(\pi^+\pi^-)$ distribution is consistent with
 146 the result of phase-space decay simulation, with $\chi^2/\text{ndf} = 1.6$ for $\text{ndf} = 9$. No peaking
 147 structures are evident.

148 Systematic uncertainties on the mass measurement are shown in Table 1. The
 149 dominant uncertainty in the absolute A_b^{*0} mass measurement comes from the uncer-
 150 tainty on the A_b^0 mass $\delta M_{A_b^0} = 0.69$ MeV/ c^2 ; it is propagated to the A_b^{*0} mass un-
 151 certainty as $\delta M_{A_b^{*0}} = \delta M_{A_b^0} \times (M_{A_b^0}/M_{A_b^{*0}}) \simeq 0.66$ MeV/ c^2 . This uncertainty mostly

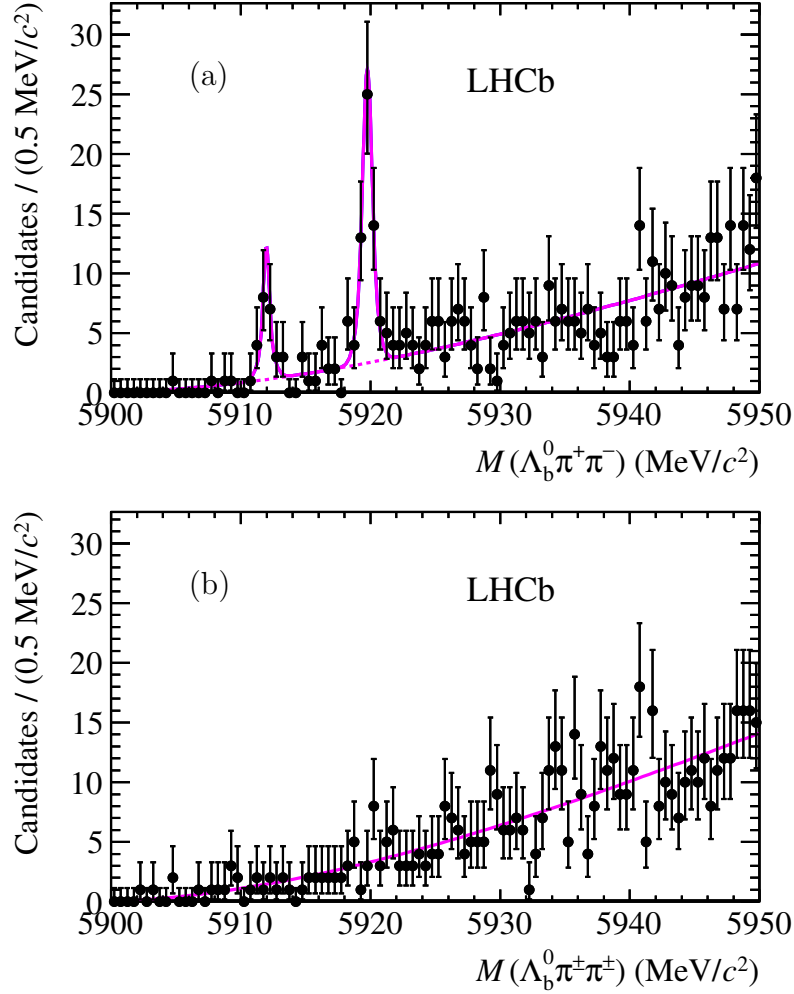


Figure 2: Invariant mass spectrum of (a) $\Lambda_b^0 \pi^+ \pi^-$ and (b) $\Lambda_b^0 \pi^\pm \pi^\pm$ combinations. The points with error bars are the data, the solid line is the fit result, the dashed line is the background contribution.

152 cancels in the mass difference $\Delta M_{\Lambda_b^{*0}} = M_{\Lambda_b^{*0}} - M_{\Lambda_b^0}$, where the residual uncertainty is
 153 $\delta \Delta M_{\Lambda_b^{*0}} = \delta M_{\Lambda_b^0} \times (\Delta M_{\Lambda_b^0} / M_{\Lambda_b^{*0}})$. The uncertainty of the signal parameterization is es-
 154 timated by using the simulated signal parameterization without applying the resolution
 155 scaling factor, by using the natural width for both states when left free in the fit, and by
 156 conservatively including the $\Lambda_b^0 \rightarrow \Lambda_c^+ K^-$ contribution with the rate 12% parameterized
 157 from simulation. The uncertainty due to the background parameterization is estimated
 158 by:

- 159 • using an alternative fit model for background description,
- 160 • using the fit without the $\Lambda_b^0 \pi^\pm \pi^\pm$ constraint,
- 161 • using the fit with the background obtained from the simulation,

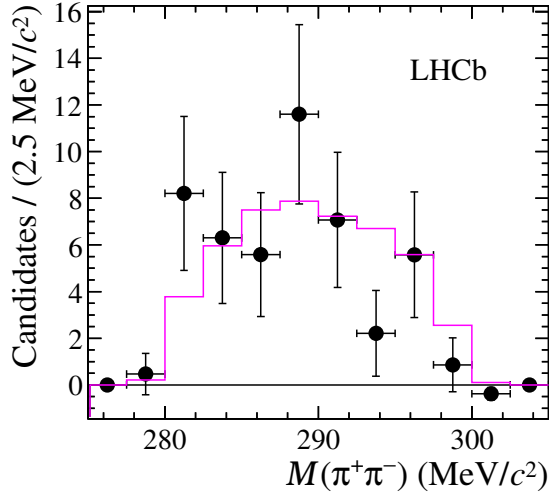


Figure 3: Invariant mass of the two pions from $\Lambda_b^{*0}(5920) \rightarrow \Lambda_b^0 \pi^+ \pi^-$ decay. The points with the error bars are background-subtracted data, the solid histogram is the result of phase-space decay simulation.

Table 1: Systematic uncertainties on the mass difference $\Delta M_{\Lambda_b^{*0}}$ between Λ_b^{*0} and Λ_b^0 .

Source of uncertainty	Systematic bias, MeV/c^2	
	$\Delta M_{\Lambda_b^{*0}(5912)}$	$\Delta M_{\Lambda_b^{*0}(5920)}$
Λ_b^0 mass	0.034	0.035
Signal PDF	0.021	0.011
Background PDF	0.002	0.002
Momentum scale	0.008	0.013
Total	0.041	0.039

162 • fitting in the reduced invariant mass range 5910–5930 MeV/c^2 ,

163 and taking the largest difference from the nominal fit result as systematic uncertainty.
 164 The effect of the momentum scale correction is evaluated by varying the scale coefficient
 165 by its relative uncertainty 5×10^{-4} in simulated signal samples.

166 The significance of the observation of the two states is evaluated with simulated
 167 pseudo-experiments. A large number of background-only invariant mass distributions
 168 are simulated with parameters equal to the fit result, and each distribution is fitted with
 169 models that include background only, as well as background and signal. The mean mass
 170 value of the signal PDF is not constrained in the fit to account for a trial factor in the
 171 range 5900–5950 MeV/c^2 . The significance is calculated as the fraction of samples where

172 the difference of the logarithms of fit likelihoods $\Delta \log \mathcal{L}$ with and without the signal
 173 is larger than in data. The fraction is obtained by an exponential extrapolation of the
 174 $\Delta \log \mathcal{L}$ distribution [28] that allows a limited number of pseudo-experiments to be used
 175 for a signal with high significance. The significance is then expressed in terms of the
 176 number of standard deviations (σ). The significance of the $\Lambda_b^{*0}(5912)$ state obtained in
 177 this way is 5.4σ for the $\Delta \log \mathcal{L}$ obtained from the nominal fit. To account for systematic
 178 effects, the minimum $\Delta \log \mathcal{L}$ among all systematic variations is taken; in that case the
 179 significance reduces to 5.2σ . Similarly, the statistical significance of the $\Lambda_b^{*0}(5920)$ state
 180 is 11.7σ , and the significance including systematic uncertainties is 10.2σ .

181 The fit biases and the validity of the statistical uncertainties are checked with pseudo-
 182 experiments where the PDF contains both signal and background components. The fit
 183 does not introduce any noticeable bias on the measurement of the masses. The mass
 184 uncertainty for $\Lambda_b^{*0}(5920)$ state is estimated correctly within 1% precision; however, the
 185 mass uncertainty for the $\Lambda_b^{*0}(5912)$ is underestimated by 4%. This factor is taken into
 186 account in the final result.

187 In summary, we report the observation of two narrow states in the $\Lambda_b^0 \pi^+ \pi^-$ mass
 188 spectrum, $\Lambda_b^{*0}(5912)$ and $\Lambda_b^{*0}(5920)$, with masses

$$M_{\Lambda_b^{*0}(5912)} = 5911.97 \pm 0.12 \pm 0.02 \pm 0.66 \text{ MeV}/c^2,$$

$$M_{\Lambda_b^{*0}(5920)} = 5919.77 \pm 0.08 \pm 0.02 \pm 0.66 \text{ MeV}/c^2,$$

189 where the first uncertainty is statistical, the second is systematic, and the third is the
 190 uncertainty due to knowledge of the Λ_b^0 mass. The values of the mass differences with
 191 respect to the Λ_b^0 mass, where most of the last uncertainty cancels, and the remaining
 192 part is included in the systematic uncertainty, are

$$\Delta M_{\Lambda_b^{*0}(5912)} = 292.60 \pm 0.12(\text{stat}) \pm 0.04(\text{syst}) \text{ MeV}/c^2,$$

$$\Delta M_{\Lambda_b^{*0}(5920)} = 300.40 \pm 0.08(\text{stat}) \pm 0.04(\text{syst}) \text{ MeV}/c^2.$$

193 The signal yield for the $\Lambda_b^{*0}(5912)$ state is 17.6 ± 4.8 events, and the significance of
 194 the signal (including systematic uncertainty and trial factor in the mass range 5900–
 195 5950 MeV/c^2) is 5.2 standard deviations. For the $\Lambda_b^{*0}(5920)$ state, the yield is 52.5 ± 8.1
 196 events and the significance is 10.2 standard deviations. The limits on the natural widths of
 197 these states are $\Gamma_{\Lambda_b^{*0}(5912)} < 0.66 \text{ MeV}$ ($< 0.83 \text{ MeV}$) and $\Gamma_{\Lambda_b^{*0}(5920)} < 0.63 \text{ MeV}$ (< 0.75)
 198 at the 90% (95%) CL.

199 The masses of Λ_b^{*0} states obtained in our analysis are 30–40 MeV/c^2 higher than in
 200 the prediction using the constituent quark model [12], and 20–30 MeV/c^2 lower than the
 201 predictions based on the relativistic quark model [11], modeling the color hyperfine inter-
 202 action [14] and an approach based on the heavy quark effective theory [15]. Calculation
 203 involving a combined heavy quark and large number of colors expansion [9, 10] gives a
 204 value roughly in agreement, although only the spin-averaged prediction is available. The
 205 earlier prediction based on the relativized quark potential model [13] matches well the
 206 absolute mass values for both states, but the Λ_b^0 mass prediction using this model is
 207 35 MeV/c^2 lower than the measured value.

208 We express our gratitude to our colleagues in the CERN accelerator departments for
 209 the excellent performance of the LHC. We thank the technical and administrative staff at
 210 CERN and at the LHCb institutes, and acknowledge support from the National Agencies:
 211 CAPES, CNPq, FAPERJ and FINEP (Brazil); CERN; NSFC (China); CNRS/IN2P3
 212 (France); BMBF, DFG, HGF and MPG (Germany); SFI (Ireland); INFN (Italy); FOM
 213 and NWO (The Netherlands); SCSR (Poland); ANCS (Romania); MinES of Russia and
 214 Rosatom (Russia); MICINN, XuntaGal and GENCAT (Spain); SNSF and SER (Switzer-
 215 land); NAS Ukraine (Ukraine); STFC (United Kingdom); NSF (USA). We also acknowl-
 216 edge the support received from the ERC under FP7 and the Region Auvergne.

217 References

- 218 [1] D0 collaboration, V. Abazov *et al.*, *Direct observation of the strange b baryon Ξ_b^-* ,
 219 *Phys. Rev. Lett.* **99** (2007) 052001, [arXiv:0706.1690](#).
- 220 [2] CDF collaboration, T. Aaltonen *et al.*, *Observation and mass measurement of the*
 221 *baryon Ξ_b^-* , *Phys. Rev. Lett.* **99** (2007) 052002, [arXiv:0707.0589](#).
- 222 [3] D0 collaboration, V. Abazov *et al.*, *Observation of the doubly strange b baryon Ω_b^-* ,
 223 *Phys. Rev. Lett.* **101** (2008) 232002, [arXiv:0808.4142](#).
- 224 [4] CDF collaboration, T. Aaltonen *et al.*, *Observation of the Ω_b^- baryon and measure-*
 225 *ment of the properties of the Ξ_b^- and Ω_b^- baryons*, *Phys. Rev.* **D80** (2009) 072003,
 226 [arXiv:0905.3123](#).
- 227 [5] CDF collaboration, T. Aaltonen *et al.*, *Observation of the Ξ_b^0 baryon*, *Phys. Rev.*
 228 *Lett.* **107** (2011) 102001, [arXiv:1107.4015](#).
- 229 [6] CMS Collaboration, S. Chatrchyan *et al.*, *Observation of an excited Ξ_b baryon*,
 230 [arXiv:1204.5955](#).
- 231 [7] CDF collaboration, T. Aaltonen *et al.*, *First observation of heavy baryons Σ_b and Σ_b^** ,
 232 *Phys. Rev. Lett.* **99** (2007) 202001, [arXiv:0706.3868](#).
- 233 [8] CDF collaboration, T. Aaltonen *et al.*, *Measurement of the masses and widths of the*
 234 *bottom baryons Σ_b^\pm and $\Sigma_b^{*\pm}$* , [arXiv:1112.2808](#).
- 235 [9] Z. Aziza Baccouche, C.-K. Chow, T. D. Cohen, and B. A. Gelman, *Excited heavy*
 236 *baryons and their symmetries. 3. Phenomenology*, *Nucl. Phys.* **A696** (2001) 638,
 237 [arXiv:hep-ph/0105148](#).
- 238 [10] Z. Aziza Baccouche, C.-K. Chow, T. D. Cohen, and B. A. Gelman, *Model-independent*
 239 *predictions for low energy isoscalar heavy baryon observables in the combined heavy*
 240 *quark and large N_c expansion*, *Phys. Lett.* **B514** (2001) 346, [arXiv:hep-ph/0106096](#).

- 241 [11] D. Ebert, R. Faustov, and V. Galkin, *Masses of excited heavy baryons in the rela-*
242 *tivistic quark model*, Phys. Lett. **B659** (2008) 612, arXiv:0705.2957.
- 243 [12] H. Garcilazo, J. Vijande, and A. Valcarce, *Faddeev study of heavy baryon spec-*
244 *troscopy*, J. Phys. **G34** (2007) 961, arXiv:hep-ph/0703257.
- 245 [13] S. Capstick and N. Isgur, *Baryons in a relativized quark model with chromodynamics*,
246 Phys. Rev. **D34** (1986) 2809.
- 247 [14] M. Karliner, B. Keren-Zur, H. J. Lipkin, and J. L. Rosner, *The quark model and b*
248 *baryons*, Annals Phys. **324** (2009) 2, arXiv:0804.1575.
- 249 [15] W. Roberts and M. Pervin, *Heavy baryons in a quark model*, Int. J. Mod. Phys. **A23**
250 (2008) 2817, arXiv:0711.2492.
- 251 [16] LHCb collaboration, A. A. Alves Jr. *et al.*, *The LHCb detector at the LHC*, JINST
252 **3** (2008) S08005.
- 253 [17] V. Gligorov, C. Thomas, and M. Williams, *The HLT inclusive B triggers*, LHCb-
254 PUB-2011-016.
- 255 [18] Particle Data Group, K. Nakamura *et al.*, *Review of particle physics*, J. Phys. **G37**
256 (2010) 075021.
- 257 [19] LHCb Collaboration, R. Aaij *et al.*, *Measurement of b-hadron masses*, Phys. Lett.
258 **B708** (2012) 241, arXiv:1112.4896.
- 259 [20] T. Sjöstrand, S. Mrenna, and P. Skands, *PYTHIA 6.4 Physics and manual*, JHEP
260 **05** (2006) 026, arXiv:hep-ph/0603175.
- 261 [21] I. Belyaev *et al.*, *Handling of the generation of primary events in GAUSS, the LHCb*
262 *simulation framework*, Nuclear Science Symposium Conference Record (NSS/MIC)
263 **IEEE** (2010) 1155.
- 264 [22] D. J. Lange, *The EvtGen particle decay simulation package*, Nucl. Instrum. Meth.
265 **A462** (2001) 152.
- 266 [23] P. Golonka and Z. Was, *PHOTOS Monte Carlo: a precision tool for QED corrections*
267 *in Z and W decays*, Eur. Phys. J. **C45** (2006) 97, arXiv:hep-ph/0506026.
- 268 [24] GEANT4 collaboration, J. Allison *et al.*, *Geant4 developments and applications*,
269 IEEE Trans. Nucl. Sci. **53** (2006) 270; GEANT4 collaboration, S. Agostinelli *et al.*,
270 *GEANT4: A simulation toolkit*, Nucl. Instrum. Meth. **A506** (2003) 250.
- 271 [25] M. Clemencic *et al.*, *The LHCb Simulation Application, Gauss: Design, Evolution*
272 *and Experience*, J. of Phys: Conf. Ser. **331** (2011) 032023.

- 273 [26] LHCb collaboration, R. Aaij *et al.*, *Measurement of b -hadron masses*, Phys. Lett.
274 **B708** (2012) 241, [arXiv:1112.4896](#).
- 275 [27] M. Pivk and F. L. Diberder, *sPlot: A statistical tool to unfold data distributions*,
276 Nucl. Instrum. Meth. **A555** (2005) 356, [arXiv:physics/0402083](#).
- 277 [28] E. Gross and O. Vitells, *Trial factors for the look elsewhere effect in high energy*
278 *physics*, Eur. Phys. J. **C70** (2010) 525, [arXiv:1005.1891](#).